AN IMPROVED VARIATIONAL MODE DECOMPOSITION METHOD FOR INTERNAL WAVES SEPARATION

Jeremy Schmitt, Ernesto Horne, Nelly Pustelnik, Sylvain Joubaud, Philippe Odier

Laboratoire de Physique de l'Ecole Normale Supérieure de Lyon, UMR CNRS 5672, F-69364 Lyon, France,

firstname.lastname@ens-lyon.fr

ABSTRACT

This paper proposes to revisit the 2-D Variational Mode Decomposition (2-D–VMD) in order to separate the incident and reflected waves in experimental images of internal waves velocity field. 2-D–VMD aims at splitting an image into a sequence of oscillating components which are centered around specific spatial frequencies. In this work we develop a proximal algorithm with local convergence guarantees, allowing more flexibility in order to deal with modes having different spectral properties and to add some optional constraints modeling prior informations. Our method is compared with the standard 2-D–VMD and with a Hilbert based strategy usually employed for processing internal waves images.

Index Terms— Optimisation, mode decomposition, internal waves.

1. INTRODUCTION

The aim of this study is to extract reflecting and incident waves from experimental images modeling the velocity field of oceanic internal wave reflection. Internal waves are waves propagating in the bulk of a fluid whose density varies with depth (ocean, atmosphere, interior of stars) [1]. Due to their intrinsic properties, these waves, as they reflect upon an inclined slope, can undergo a strong focalization [2]. An experiment designed to study this phenomenon consists in observing the waves through a measurement of the fluid velocity [3]. The main challenge in this study is to separate the incident and reflected waves, which have the same temporal frequency. The incident wave is localized in the spatial Fourier spectrum, while the reflected wave is not. The classical procedure to perform this separation is based on a Hilbert transform [4] but it fails to achieve this separation properly by introducing some boundary artefacts and undesirable oscillations.

This question can be formulated as an inverse problem that consists in extracting K oscillating components, denoted $(\mathbf{u}_k)_{1\leq k\leq K}$ with $\mathbf{u}_k \in \mathbb{R}^{N_1\times N_2}$, from the observed data $\mathbf{z} \in \mathbb{R}^{N_1\times N_2}$ such that

$$\mathbf{z} = \sum_{k=1}^{K} \mathbf{u}_k + \varepsilon,$$

where ε models an additive noise. The study of internal wave reflection corresponds to the specific case $K = 2$, where $\mathbf{z}$ models the velocity field, and each component is centered around an unknown frequency $\boldsymbol{\omega}_k = (\omega_{k,1}, \omega_{k,2})$ so that, for every location $(\ell_1, \ell_2) \in \{1, \dots, N_1\} \times \{1, \dots, N_2\}$,

$$u_{k,(\ell_1,\ell_2)} = a_{k,(\ell_1,\ell_2)} \cos\big(v_{k,1,(\ell_1,\ell_2)}\ell_1 + v_{k,2,(\ell_1,\ell_2)}\ell_2 + \varphi\big),$$

where $\mathbf{a}_k \in \mathbb{R}^{N_1\times N_2}$ models the amplitude changes and, for $i \in \{1, 2\}$, the mean value of $\mathbf{v}_{k,i} \in \mathbb{R}^{N_1\times N_2}$ is close to $\omega_{k,i}$, and φ is a phase term.

In the recent literature of component extraction for image analysis, efficient methods are 2-D synchrosqueezing [5] or 2-D empirical mode decomposition [6]. The drawback of the first one is to require a supervised domain selection in order to extract each component while the second one may suffer lack of robustness when noise is involved. Another strategy has been proposed in [7] based on monogenic analysis and in [8] for estimating jointly $(\mathbf{u}_k)_{1\leq k\leq K}$ and $(\boldsymbol{\omega}_k)_{1\leq k\leq K}$. However, all these four methods are not designed to extract components that can be spread out on the frequency spectrum in one direction. In this work, we propose to revisit the work by Dragomirestkiy and Zosso, initially formulated for analyzing 1-D signals [9] and extended to image analysis in [8], in order to incorporate constraints imposed by internal waves analysis.

In section 2, we focus on the design of a new criterion adapted to the problem of extracting reflecting and incident waves from velocity field data. In Section 3, we derive an algorithm solving the associated minimization problem insuring some local convergence guarantees and in Section 4, experimental results demonstrate the efficiency of the proposed method compared to state-of-the-art strategies. A conclusion is drawn in Section 5.

Notation A matrix in $\mathbb{R}^{N_1\times N_2}$ is denoted in bold as $\mathbf{u}$ and its components are $(u_{(\ell_1,\ell_2)\in\mathcal{L}})$ with $\mathcal{L} = \{1, \dots, N_1\} \times \{1, \dots, N_2\}$. The Fourier transform of the image $\mathbf{u}$ is denoted $\hat{\mathbf{u}}$ and the frequency indices are $(\nu_1, \nu_2) \in \mathcal{V} = \{\lfloor -N_1/2\rfloor, \dots, \lfloor N_1/2\rfloor\} \times \{\lfloor -N_2/2\rfloor, \dots, \lfloor N_2/2\rfloor\}$.

This work is supported by the ANR-13-BS03-0002 ASTRES grant and ANR-11-BS04-006-01 ONLITUR

2. CRITERION

The solution proposed in [8] aims to estimate jointly $(\mathbf{u}_k)_{1\leq k\leq K}$ and $(\boldsymbol{\omega}_k)_{1\leq k\leq K}$ by solving

$$\min_{(\mathbf{u}_k,\boldsymbol{\omega}_k)_{1\leq k\leq K}} \Big\{ \Big\| \mathbf{z} - \sum_{k=1}^{K} \mathbf{u}_k \Big\|_2^2 + \alpha \sum_{k=1}^{K} \Big\| D\big(u^{AS}_{k,(\ell_1,\ell_2)} e^{-j(\omega_{k,1}\ell_1+\omega_{k,2}\ell_2)}\big)_{(\ell_1,\ell_2)\in\mathcal{L}} \Big\|_2^2 \Big\}, \quad (1)$$

,where the 2D analytic signal $\mathbf{u}_k^{AS}$ is defined in the Fourier domain, for every frequency $(\nu_1,\nu_2)\in\mathcal{V}$, as

$$\widehat{u}^{AS}_{k,(\nu_1,\nu_2)} = (1+\mathrm{sign}(\omega_{k,1}\nu_1+\omega_{k,2}\nu_2))\widehat{u}_{k,(\nu_1,\nu_2)}.$$

The 2D analytic signal is chosen to set to zero one half-plane of the frequency domain relatively to the frequency vector $\boldsymbol{\omega}_k$. D models the gradient operator and the coefficient $\alpha>0$ denotes a regularization parameter allowing to adjust the selectivity of the filter.

The limitations related to this criterion are essentially twofold. First, incident and reflected wave have different spectral behaviors. In particular, the spectrum of the reflected wave is very compact horizontally but not vertically. We introduce parameters $\alpha_{k,i}$, depending of the mode k and the coordinate $i\in\{1,2\}$, in order to separately adjust the horizontal and vertical spectral compacity of each mode. Second, we would like to add some prior information linked to the physics of internal waves. In particular, the reflected wave only propagates along the reflection slope and it is null far away from the slope. This prior information can be introduced by means of a penalty term $f_k(\mathbf{u}_k)$. For instance it can be chosen as an indicator function $i_C(\mathbf{u}_k)$ whose value is 0 if $\mathbf{u}_k\in C=\big\{\mathbf{u}\in\mathbb{R}^N \,|\, (\forall(\ell_1,\ell_2)\in\mathcal{S}) \quad u_{(\ell_1,\ell_2)}=0\big\}$ and $+\infty$ otherwise. For such a choice of the penalty f_k, we impose the component $\mathbf{u}_k$ to be zero in the set of indices $\mathcal{S}$. Such a choice of C denotes a non-empty, closed and convex subset of $\mathbb{R}^{N_1\times N_2}$. But more generally, we assume that f_k is at least convex, lower semi-continuous and proper from $\mathbb{R}^{N_1\times N_2}$ to $]-\infty,+\infty]$.

According to previous remarks, the criterion we derive is:

$$\min_{\mathbf{u}_k,\boldsymbol{\omega}_k} \Big\{ \sum_k f_k(\mathbf{u}_k) + \lambda \Big\| \sum_k \mathbf{u}_k - \mathbf{z} \Big\|_2^2 + \sum_k \alpha_{k,1} \Big\| D_1\big(u^{AS}_{k,(\ell_1,\ell_2)} e^{-j\omega_{k,1}\ell_1}\big)_{(\ell_1,\ell_2)\in\mathcal{L}} \Big\|_2^2 + \sum_{k=1}^{K} \alpha_{k,2} \Big\| D_2\big(u^{AS}_{k,(\ell_1,\ell_2)} e^{-j\omega_{k,2}\ell_2}\big)_{(\ell_1,\ell_2)\in\mathcal{L}} \Big\|_2^2 \Big\}, \quad (2)$$

where D_1 and D_2 denote respectively the horizontal and vertical gradient operator. The parameters $\alpha_{k,1}$ and $\alpha_{k,2}$ allowing to adjust the selectivity are chosen positive. The parameter λ allows us to adjust the fidelity to data. Similarly to (1), this criterion is also non-convex. In what follows, we propose an algorithmic solution to estimate a local minimizer.

3. ALGORITHM

A popular approach for solving (2) consists in alternating the minimization over $(\mathbf{u}_k)_{1\leq k\leq K}$ and $(\boldsymbol{\omega}_k)_{1\leq k\leq K}$. For every iterations $m\geq 1$ and each mode $k\in\{1,\dots,K\}$, we denote

$$\phi_{k,m}(\mathbf{u}) = f_k(\mathbf{u}) + \lambda\|\mathbf{u} + \sum_{i\neq k}\mathbf{u}_i^{[m]} - \mathbf{z}\|_2^2 + \alpha_{k,1}\Big\| D_1\big(u^{AS}_{(\ell_1,\ell_2)} e^{-j\omega_{k,1}^{[m]}\ell_1}\big)_{(\ell_1,\ell_2)\in\mathcal{L}} \Big\|_2^2 + \alpha_{k,2}\Big\| D_2\big(u^{AS}_{(\ell_1,\ell_2)} e^{-j\omega_{k,2}^{[m]}\ell_2}\big)_{(\ell_1,\ell_2)\in\mathcal{L}} \Big\|_2^2, \quad (3)$$

$$\psi_{k,m}(\boldsymbol{\omega}) = \alpha_{k,1}\Big\| D_1\big(u^{AS,[m+1]}_{k,(\ell_1,\ell_2)} e^{-j\omega_1\ell_1}\big)_{(\ell_1,\ell_2)\in\mathcal{L}} \Big\|_2^2 + \alpha_{k,2}\Big\| D_2\big(u^{AS,[m+1]}_{k,(\ell_1,\ell_2)} e^{-j\omega_2\ell_2}\big)_{(\ell_1,\ell_2)\in\mathcal{L}} \Big\|_2^2. \quad (4)$$

Based on this functions, an alternating procedure is summarized in Algorithm 1.

Algorithm 1 Gauss-Seidel algorithm

For $m=1,2,\dots$
  For $k=1,\dots,K$
    $\mathbf{u}_k^{[m+1]} \in \underset{\mathbf{u}\in\mathbb{R}^{N_1\times N_2}}{\mathrm{Argmin}}\ \phi_{k,m}(\mathbf{u})$
    $\boldsymbol{\omega}_k^{[m+1]} \in \underset{\boldsymbol{\omega}\in\mathbb{R}^2}{\mathrm{Argmin}}\ \psi_{k,m}(\boldsymbol{\omega})$

This algorithmic strategy is used in [8] when $\alpha=\alpha_{k,1}=\alpha_{k,2}$ and $f_k=0$. For this configuration, such a minimization strategy provides satisfactory results however it involves parameters tricky to adjust. Moreover, it is well known that such an alternating minimization procedure requires restrictive conditions to guarantee convergence to a local minimizer as discussed in [10, 11]. A simple solution to overcome these difficulties is to replace each minimisation step by a proximity operator step as suggested in [11] and described in Algorithm 2. Algorithm 2 has attractive convergence properties. The convergence to a global minimum is ensured in the case where the criterion is coercive and semi-algebraic [11].

Algorithm 2 Proximal alternating algorithm

Set $\mu>0$ and $\rho>0$
For $m=1,2,\dots$
  For $k=1,\dots,K$
    $\mathbf{u}_k^{[m+1]} = \underset{\mathbf{u}\in\mathbb{R}^{N_1\times N_2}}{\arg\min}\ \phi_{k,m}(\mathbf{u}) + \frac{1}{2\rho}\|\mathbf{u}-\mathbf{u}_k^{[m]}\|_2^2$
    $\boldsymbol{\omega}_k^{[m+1]} = \underset{\boldsymbol{\omega}\in\mathbb{R}^2}{\arg\min}\ \psi_{k,m}(\boldsymbol{\omega}) + \frac{1}{2\mu}\|\boldsymbol{\omega}-\boldsymbol{\omega}_k^{[m]}\|_2^2$

In order to solve each step efficiently, we rewrite them in the Fourier domain. We denote F the Fourier transform and F^{-1} the inverse Fourier transform. Due to the Parseval/Plancherel theorem, both subproblems can be written in

the Fourier domain:

$$\hat{\mathbf{u}}_k^{[m+1]} = \arg\min_{\hat{\mathbf{u}}} \frac{1}{2\rho}\Bigg\{ \|\hat{\mathbf{u}}_k^{[m]} - \hat{\mathbf{u}}\|_2^2 + f_k(F^{-1}\hat{\mathbf{u}}) + \lambda\|\hat{\mathbf{u}} + \sum_{i\neq k}\hat{\mathbf{u}}_i^{[m]} - \hat{\mathbf{z}}\|_2^2 + \alpha_{k,1}\Big\|\Big(j(\nu_1-\omega_{k,1}^{[m]})(1+\mathrm{sign}(\nu_1))\hat{u}_{(\nu_1,\nu_2)}\Big)_{(\nu_1,\nu_2)\in\mathcal{V}}\Big\|_2^2 + \alpha_{k,2}\Big\|\Big(j(\nu_2-\omega_{k,2}^{[m]})(1+\mathrm{sign}(\nu_2))\hat{u}_{(\nu_1,\nu_2)}\Big)_{(\nu_1,\nu_2)\in\mathcal{V}}\Big\|_2^2\Bigg\},$$

$$\boldsymbol{\omega}_k^{[m+1]} = \arg\min_{\boldsymbol{\omega}\in\mathbb{R}^2}\Bigg\{ \frac{1}{2\mu}\|\boldsymbol{\omega}_k^{[m]} - \boldsymbol{\omega}\|_2^2 + \alpha_{k,1}\Big\|\Big(j(\nu_1-\omega_1)(1+\mathrm{sign}(\nu_1))\hat{u}_{k,(\nu_1,\nu_2)}^{[m+1]}\Big)_{(\nu_1,\nu_2)\in\mathcal{V}}\Big\|_2^2 + \alpha_{k,2}\Big\|\Big(j(\nu_2-\omega_2)(1+\mathrm{sign}(\nu_2))\hat{u}_{k,(\nu_1,\nu_2)}^{[m+1]}\Big)_{(\nu_1,\nu_2)\in\mathcal{V}}\Big\|_2^2\Bigg\}.$$

The estimation step of $\boldsymbol{\omega}_k^{[m+1]}$ has an analytic expression that is, for every $i \in \{1,2\}$,

$$\omega_{k,i}^{[m+1]} = \frac{\omega_{k,i}^{[m]} + 8\mu\alpha_{k,i}\sum_{(\nu_1,\nu_2)\in\Omega_k^{[m]}}\nu_i\big(\hat{u}_{k,(\nu_1,\nu_2)}^{[m+1]}\big)^2}{1 + 8\mu\alpha_{k,i}\sum_{(\nu_1,\nu_2)\in\Omega_k^{[m]}}\big(\hat{u}_{k,(\nu_1,\nu_2)}^{[m+1]}\big)^2}, \tag{5}$$

where $\Omega_k^{[m]}$ denotes the half-plane in the Fourier domain:

$$\Omega_k^{[m]} = \{\boldsymbol{\nu} = (\nu_1,\nu_2) \in \mathcal{V} \mid \nu_1\omega_{k,1}^{[m]} + \nu_2\omega_{k,2}^{[m]} \geqslant 0\}.$$

On the other hand, the estimation of $\mathbf{u}_k^{[m+1]}$ is obtained through forward-backward iterations generating a sequence $(\mathbf{v}_k^{[p]})_{p\geq 0}$ build as

$$v_k^{[p+1]} = \mathrm{prox}_{\gamma\rho f_k}\big(v_k^{[p]} + \gamma\mathbf{b} - \gamma F^{-1}AF\mathbf{v}_k^{[p]}\big), \tag{6}$$

where the proximity operator step allows us to deal with the non-smooth function f_k. It is defined as

$$(\forall x \in \mathbb{R}^{N_1\times N_2}) \quad \mathrm{prox}_{f_k}x = \arg\min_y f_k(y) + \frac{1}{2}\|x-y\|_2^2,$$

which is reduced to the projection onto a closed convex set when $f_k = \iota_C$. In (6), A models a linear operator defined as

$$A\colon \hat{\mathbf{u}} \to \begin{cases} A_{(\nu_1,\nu_2)}\hat{u}_{(\nu_1,\nu_2)} & \text{if} \quad (\nu_1,\nu_2)\in\Omega_k^{[m]}, \\ 0 & \text{otherwise,}\end{cases}$$

with

$$A_{(\nu_1,\nu_2)} = 1+2\rho\lambda+4\rho(\alpha_{k,1}(\nu_1-\omega_{k,1})^2+\alpha_{k,2}(\nu_2-\omega_{k,2})^2)$$

and $\mathbf{b} \in \mathbb{R}^{N_1\times N_2}$ is such that

$$b_{(\ell_1,\ell_2)} = u_{k,(\ell_1,\ell_2)}^{[m]} + 2\rho\lambda(z_{(\ell_1,\ell_2)} - \sum_{i\neq k}u_{i,(\ell_1,\ell_2)}^{[m]})$$

The iterations are summarized in Algorithm 3.

Algorithm 3 Prox-2D-VMD algorithm

Choose the parameters $\lambda > 0$, $\rho > 0$, $\mu > 0$
Set the parameters $\alpha_{k,1} > 0$, $\alpha_{k,2} > 0$
Initialize $\big(\mathbf{u}_k^{[1]}\big)_{1\leq k\leq K}$, $\big(\boldsymbol{\omega}_k^{[1]}\big)_{1\leq k\leq K}$
For every $m = 1, 2, \ldots$
  For every $k \in \{1,\ldots,K\}$
    Set $\mathbf{v}_k^{[1]} = \mathbf{u}_k^{[m]}$
    Set $\gamma \in \left]0; 2/\|A\|\right[$
    For $p = 0, 1, \ldots$
    Update $\mathbf{v}_k^{[p]}$ as detailled in (6)
    Set $\mathbf{u}_k^{[m+1]} = \lim_{p\to+\infty}\mathbf{v}_k^{[p]}$
  Compute $\omega_{k,1}^{[m+1]}$ and $\omega_{k,2}^{[m+1]}$ using (5)

4. EXPERIMENTAL RESULTS

Experiments are performed on a critical reflection velocity field image $\mathbf{z}$ of size $N_1 = 132$ and $N_2 = 238$ illustrated on Fig.1(a). Our goal is to extract the incident wave and the reflected wave (thus, $K = 2$) from $\mathbf{z}$. Our method is compared with a method based on Hilbert-transform, which is usually used to process the internal waves velocity field [4] and with the 2-D–VMD proposed in [8] where the data fidelity constraint is enforced strictly through an augmented Lagrangian. An illustration of each strategy is illustrated in Fig.1. One can observe that the Hilbert based strategy leads to mode mixing, while the standard 2-D–VMD provides undesirables oscillations in the top of the 2-D field. The proposed method removes all these artefacts.

In order to evaluate the impact of the proposed constraints, we perform three different experiments. In the first experiment, there is no optional constraint ($f_1 = f_2 = 0$) and no directionality ($\alpha_{k,i} \equiv \alpha$). In the second experiment, we add the directionality constraint for the second component by setting $\alpha_{2,2} = \alpha/2$, since the spectrum of the reflected wave is expected to be more spread out horizontally than vertically. In the third experiment, we combine the directionality with the zero constraint by setting $\mathcal{S}$ to be the top first 70 rows of $\mathbf{u}_2$ ($\alpha_{2,2} = \alpha/2$ and $f_2 = i_C$). The results are illustrated in Figure 2, which shows mean vertical profiles of the incident wave $\mathbf{u}_1$ (solid line) and the reflected wave $\mathbf{u}_2$ (dashed line). Mean profiles are obtained by averaging the absolute value on each row of the images. In each plot, we compare the proposed solution with the ones obtained with the Hilbert filtering and 2-D–VMD. The left column presents the results of the proposed method where α is fixed and λ varies. On the right column, λ is fixed and α varies.

In the first experiment, we can observe that for larger λ, the solution is closer to the standard 2-D–VMD that imposes the exact equality between the data and the extracted components. Here, varying λ allows us some flexibility, for instance when noise is involved. A similar behaviour is observed regarding the parameter α. One can observe that the basic Hilbert filtering strongly attenuates the incident wave

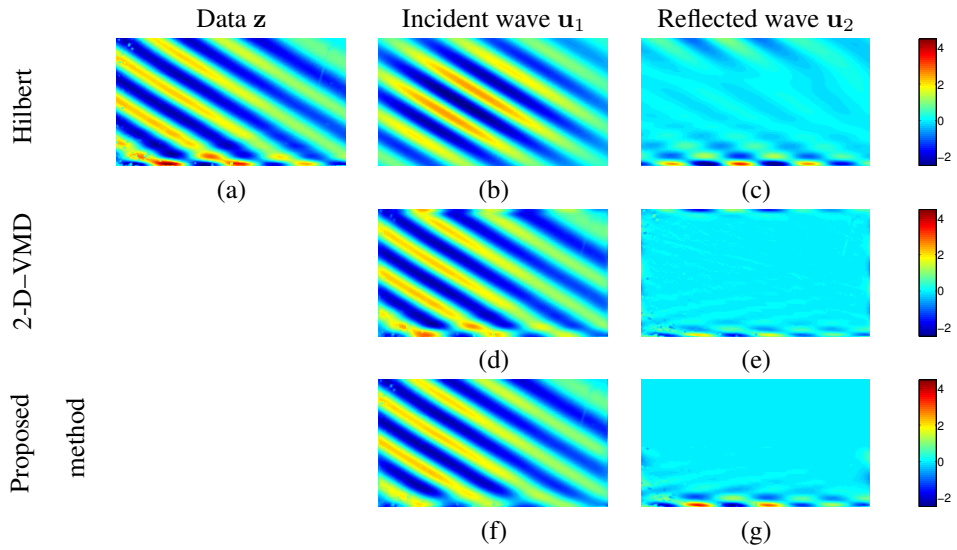

Fig. 1. Results on internal waves velocity field with critical wave reflection. 1st row: results obtained through a temporal and spatial Hilbert filtering. 2nd row: 2-D–VMD. 3rd row: proposed method with $\alpha_{2,2} = \alpha/2$ and zero value constraint on the 70 first rows of mode 2 ($f_2 = i_{\mathrm{C}}$).

on the boundaries and leads to undesirable oscillations on the reflected wave.

In the second experiment, the directionality constraint allows us to reduce the oscillations of the first IMF on the first 30 pixels near the slope. Moreover, adding this flexibility in the directionality allows us to be less sensitive to the choices of λ and α, which is why the profiles for different values of parameters are superposed. In the third experiment, we illustrate that the zero-constraint on the pixels of the second component which are far from the slope enables to cancel the undesired oscillations of the reflected wave and the boundary effects.

In our experiments, we observe that 1000 iterates are enough to insure convergence. Without the zero constraint, the convergence of the algorithm is fast (about 3 seconds) while with a zero constraint, the convergence is close to 10 minutes (since the computation of the modes $\mathbf{u}_k$ involves forward-backward iterations). In our experiments, the $\mathbf{u}_k^{[1]}$ are set to zero, while the $\boldsymbol{\omega}_k^{[1]}$ are initialized on the unit circle. however, we observe that the initialization of the $\mathbf{u}_k$ and $\boldsymbol{\omega}_k$ have no incidence on the final estimate.

5. CONCLUSION

This paper presents an efficient method for the separation of incident and reflected wave in internal waves experimental images. This method revisits the 2-D–VMD proposed by Dragomiretskiy and Zosso by adding stronger convergence guarantees, giving more degrees of freedom for the setting of parameters and the possibility to add some prior knowledge through additional constraints. The proposed method has been tested on internal wave experimental images with critical reflection, and outperforms the classic Hilbert filtering since it strongly reduces the boundary effects and the undesired oscillations in the estimated reflected wave.

REFERENCES

[1] B. R. Sutherland, *Internal gravity waves*, Cambridge University Press, 2010.

[2] OM Phillips, *The dynamics of the upper ocean*, Cambridge University Press, 1966.

[3] G. Bordes, A. Venaille, S. Joubaud, P. Odier, and T. Dauxois, "Experimental observation of a strong mean flow induced by internal gravity waves.," *Physics of Fluids*, vol. 24, no. 8, pp. Article No. 086602, August 2012.

[4] M.J. Mercier, N.B. Garnier, and T. Dauxois, "Reflection and diffraction of internal waves analyzed with the hilbert transform," *Phys. Fluids*, vol. 20, no. 8, pp. 086601, 2008.

[5] M. Clausel, T. Oberlin, and V. Perrier, "The monogenic synchrosqueezed wavelet transform: A tool for the decomposition/demodulation of AM-FM images," *Appl. Comp. Harm. Anal.*, 2014, to appear.

[6] J. Schmitt, N. Pustelnik, P. Borgnat, P. Flandrin, and L. Condat, "A 2-D Prony-Huang transform: A new tool for 2-D spectral analysis," *IEEE Trans. Image Process.*, vol. 12, pp. 5531–5544, Oct. 2014.

[7] M. Unser, D. Sage, and D. Van De Ville, "Multiresolution monogenic signal analysis using the Riesz-Laplace wavelet transform," *IEEE Trans. Image Process.*, vol. 18, no. 11, pp. 2402–2418, November 2009.

[8] K. Dragomiretskiy and D. Zosso, "Two-Dimensional Variational Mode Decomposition," in *Energy Minimization Methods in Computer Vision and Pattern Recognition*, Hong Kong, China, January 13-16 2015.

[9] K. Dragomiretskiy and D. Zosso, "Variational Mode Decomposition," *IEEE Trans. Signal Process.*, vol. 62, no. 3, pp. 531–544, February 2014.

[10] T. F. Chan and C. K. Wong, "Convergence of the alternating minimization algorithm for blind deconvolution," *Linear Algebra Appl*, vol. 316, pp. 259–285, 2000.

[11] J. Bolte, P. L. Combettes, and J.-C Pesquet, "Alternating proximal algorithm for blind image recovery," in *Proc. Int. Conf. Image Process.*, Hong Kong, China, September 2010, pp. 1673–1676, hal-00844115.

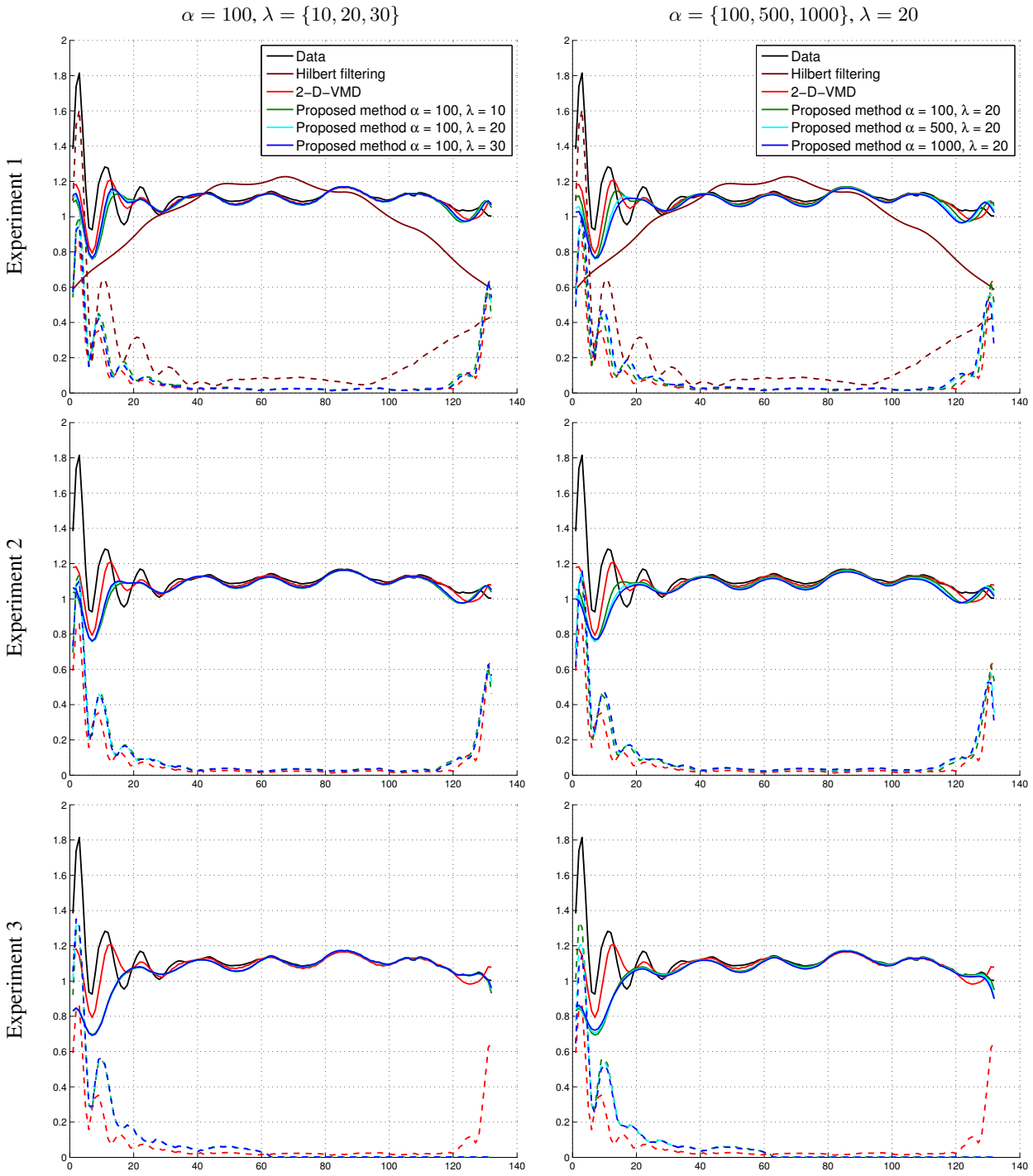

Fig. 2. Mean profile over the vertical axis of the estimates for different values of parameters α and λ. Black solid line is the mean profile of data $\mathbf{z}$. Color solid lines represent the extracted incident wave profiles with the different methods, while color dashed lines represent the extracted reflected waves profiles: brown for Hilbert filtering, red for 2-D–VMD ($\alpha = 100$), pink/blue/cyan for the proposed method. In the first column, $\lambda = 20$ and $\alpha = \{100, 500, 1000\}$. In the second column, $\alpha = 100$ and $\lambda = \{10, 20, 30\}$. First row shows the profiles estimated by our method in the unidirectional and unconstrained case. Second row presents the profiles estimated with the proposed method in the directional case ($\alpha_{2,2} = \alpha/2$). Third row shows the profiles estimated with the proposed method in the directional and constrained case ($f_2 = i_{\mathrm{C}}$).